



# Forkhead box K1 regulates the malignant behavior of gastric cancer by inhibiting autophagy

Yixuan Wang<sup>1#</sup>, Wensheng Qiu<sup>1#</sup>, Ning Liu<sup>1</sup>, Libin Sun<sup>1</sup>, Zhao Liu<sup>1</sup>, Shasha Wang<sup>1</sup>, Peng Wang<sup>2</sup>, Shihai Liu<sup>3</sup>, Jing Lv<sup>1</sup>

<sup>1</sup>Department of Oncology, the Affiliated Hospital of Qingdao University, Qingdao 266071, China; <sup>2</sup>Department of Oncology, Weifang Yidu Central Hospital, Qingzhou 262500, China; <sup>3</sup>Central Laboratory, the Affiliated Hospital of Qingdao University, Qingdao 266071, China

**Contributions:** (I) Conception and design: Y Wang; (II) Administrative support: W Qiu, S Liu, J Lv; (III) Provision of study materials or patients: All authors; (IV) Collection and assembly of data: All authors; (V) Data analysis and interpretation: All authors; (VI) Manuscript writing: All authors; (VII) Final approval of manuscript: All authors.

<sup>#</sup>These authors contributed equally to this work.

**Correspondence to:** Dr. Jing Lv. Department of Oncology, the Affiliated Hospital of Qingdao University, Qingdao 266071, China.

Email: lvjing8291@126.com; Dr. Shihai Liu. Central Laboratory, the Affiliated Hospital of Qingdao University, Qingdao 266071, China.

Email: shliumed@126.com.

**Background:** Forkhead box K1 (FOXK1) is a transcription factor that contributes to cancer development, but it is unclear how FOXK1 regulates the proliferation and migration of gastric cancer (GC) cells. The purpose of this study was to investigate the clinical significance, biological function, and molecular mechanisms of FOXK1 in GC.

**Methods:** We conducted bioinformatics assays and western blotting to assess FOXK1 expression. Then, we performed immunohistochemistry (IHC) with tissue microarrays (TMAs) to assess FOXK1 expression in order to identify an association between FOXK1 expression levels and clinical parameters. We used 5-ethynyl-2'-deoxyuridine (EdU), wound healing and Transwell assays to determine whether FOXK1 promotes malignant behaviors in GC. Furthermore, immunofluorescence staining, transmission electron microscopy and western blotting were used to verify an association between FOXK1 and autophagy.

**Results:** We observed high levels of FOXK1 expression in GC tissues, which were associated with the degree of malignancy in GC. FOXK1 promotes the malignant behavior of GC by regulating autophagy via activation of the class I phosphoinositide 3-kinase (PI3K)/AKT/mammalian target of rapamycin (mTOR) pathway and inhibition of the expression of class III PI3K.

**Conclusions:** These findings provide a new target for the comprehensive treatment of GC by highlighting the relationship between FOXK1 and malignant behaviors in GC.

**Keywords:** Forkhead box K1 (FOXK1); autophagy; gastric cancer; 3-methyladenine (3-MA)

Submitted Aug 15, 2019. Accepted for publication Nov 29, 2019.

doi: 10.21037/atm.2019.12.123

**View this article at:** <http://dx.doi.org/10.21037/atm.2019.12.123>

## Introduction

Gastric cancer (GC) is among the most prevalent forms of cancer and remains the second leading cause of cancer-related death (1). Recently, treatments for GC have substantially improved; however, due to a variety of genetic mutations and abnormal signaling pathways underlying

GC progression, GC mortality remains high (2). A better understanding of the unique molecular patterns of GC development will help researchers identify the mechanisms underlying alterations in tumor activities.

Forkhead box (FOX) transcription factors are involved in tumor development (3), embryogenesis (4) and the regulation of various physiological processes, such as cell

survival (5), oxidative stress (6), and control of lifespan (7). Forkhead box K1 (FO XK1) is a member of the FOX family of transcription factors and is commonly studied in myogenic cells (8). Recently, abnormal expression of FO XK1 was suggested to contribute to tumor development. According to Li *et al.* (9), FO XK1 regulates p21 expression and promotes the proliferation and metastasis of ovarian cancer. Haitao Xu and other scholars postulated that FO XK1 promotes glioblastoma proliferation and metastasis by inducing snail transcription (10). However, the link between FO XK1 and autophagy in GC remains unclear.

Autophagy is a process that is highly conserved throughout many organisms, but there is controversy regarding whether autophagy is associated with cell death. Autophagy inhibits tumor growth in the early stages by removing damaged organelles or proteins; however, in advanced tumors, autophagy elicits the opposite effect (11). In GC, downregulation of long noncoding RNA LINC01419 inhibits tumor cell migration and invasion and tumor growth. This phenomenon is promoted by inactivation of the PI3K/AKT1/mTOR pathway (12). At the same time, studies have shown that FO XK1 can regulate the AKT/mTOR pathway in liver cell lines (13), which suggests that autophagy and the PI3K/AKT/mTOR pathway play a key role in the malignant behavior of GC, but the role of FO XK1 in this dynamic is still unknown.

In this study, increased FO XK1 expression was significantly correlated with progression, metastasis, and adverse outcomes in patients with GC. In addition, this study revealed for the first time that FO XK1 promotes the malignant behavior of GC by inhibiting autophagy.

## Methods

### *Cells and culture conditions*

Four human GC cell lines (SGC7901, BGC823, MGC803, and HGC27) as well as the immortalized gastric mucosal cell line GES1 were obtained from the Cell Bank of the Chinese Academy of Sciences. AGS GC cells were obtained from Zhongqiao New Prefecture in Shanghai. All cells were grown in medium containing 10% fetal bovine serum (FBS; Gibco, NY, USA) and 1% penicillin-streptomycin (HyClone, Logan, UT, USA) in a standard humidified incubator.

For experiments involving 3-MA (MedChemExpress, Shanghai, China), cells were pretreated with 200  $\mu$ M 3-MA for 4 h before transfection.

### *Gene expression analysis*

We utilized Gene Expression Profiling Interactive Analysis (GEPIA; <http://gepia.cancer-pku.cn/detail.php?gene=FOXK1>) to compare gene expression in tumor and healthy tissues. We used Kaplan-Meier Plot (<http://kmplot.com/analysis/index.php?p=service&cancer=gastric>) to analyze the correlation between overall survival (OS) and FO XK1 expression in patients with GC and Database for Annotation, Visualization and Integrated Discovery (DAVID, <http://david.abcc.ncifcrf.gov/>), a public biological resource, for pathway analysis.

### *Patients and specimens*

We assessed 43 pairs of freshly frozen primary GC and matched healthy tissue samples collected at the Affiliated Hospital of Qingdao University. Samples from patients with GC from September 2016 to October 2018 who did or did not receive chemotherapy were collected for pathological assessment and analysis of progression. All individual patients were informed about the goals of this study and provided written informed consent.

### *Tissue microarrays (TMAs)*

GC tissues and matched noncancerous stomach tissues were analyzed using TMAs purchased from AMOS Scientific (Beijing, China). Forty-three tissue pairs in the TMAs were subjected to immunohistochemistry to assess FO XK1 expression.

The TMAs were independently evaluated by two investigators. The staining intensity was scored from 0 to 3 points as follows: 0, no staining; 1, weak staining; 2, moderate staining; and 3, strong staining. The percentage of positive cells was scored as follows: 0, <10% positive cells; 1, 10–35% positive cells; 2, 36–70% positive cells; and 4, >70% positive cells.

### *Cell transfection*

The FO XK1 open reading frame and 3'-untranslated region were previously cloned into pcDNA 3.1(+). AGS and MGC803 cells were cultured to 80–90% confluence and transfected with the pcDNA3.1-FO XK1 plasmid (Genechem Co., Ltd., Shanghai, China) or FO XK1 siRNA (Ribobio Co., Guangzhou, China) (*Table S1*) using Lipofectamine 3000 (Life Technologies, Shanghai, China)

according to the manufacturer's protocols. At 48 h after transfection, the experiments were conducted.

### ***RNA isolation and quantitative real-time RT-PCR***

Total RNA was extracted using TRIzol Reagent (TaKaRa, Beijing, China) and reverse transcribed into cDNA using the PrimeScript RTMaster Mix (Perfect Real Time) reagent (TaKaRa, Beijing, China) according to the manufacturer's instructions. Quantitative real-time PCR (qRT-PCR) was performed on an ABI 7500HT Fast Real-Time PCR System (Applied Biosystems, CA, USA). The 10  $\mu$ L reaction mixture consisted of SYBR GREEN PCR Master Mix (TaKaRa, Beijing, China), 500 nmol of primers and 300 ng of cDNA templates. The reaction was initially denatured at 95 °C for 5 min and then subjected to 60 cycles of 94 °C for 20 s, 60 °C for 20 s and 72 °C for 40 s. Next, the reaction temperature was increased from 72 °C to 95 °C, and the reactions were finally extended for 5 min at 72 °C before the temperature was increased at a rate of 0.1 °C/s for continuous fluorescence acquisition. Each qRT-PCR assay was repeated three times, and the cDNAs were measured in duplicate. The average fold of relative mRNA expression was determined using the  $2^{-\Delta\Delta C_t}$  method with GAPDH as an internal control. Primer sequences for qRT-PCR were as follows: FOXK1, forward 5'-GCCACAAAGGCTGGCAGAATT-3' and reverse 5'-TGGCTTCAGAGGCAGGGTCTAT-3'; class I PI3K, forward 5'-AACGAGAACGTGTGCCATTTG-3' and reverse 5'-AGAGATTGGCATGCTGTTCGAA-3'; class III PI3K, forward 5'-AGAGTTATGCGTTCTTTGCTGGC-3' and reverse 5'-GGGGTTCTAAAGGCAACGGGATA-3'; and GAPDH, 5'-TCGACAGTCA-GCCGCATCTT-3' and reverse: 5'-GAGTTAAAAGCAG-CCCTGGTG-3'.

### ***Western blot assays***

Total protein was extracted from GC cells and tumor tissues collected from nude mice. Proteins were subsequently separated on SDS-PAGE gels and then transferred to nitrocellulose membranes, which were blocked with 5% skim milk for 1 h at room temperature (RT). Primary antibodies (listed in *Table S2*) were incubated with the membranes overnight at 4 °C. The membranes were then washed three times with phosphate-buffered saline containing Tween 20 (PBST) for 15 min per wash and incubated with HRP-conjugated secondary

antibodies at RT for 2 h. After additional washes, the electrochemiluminescence (ECL) (Life Technologies, Shanghai, China) of the bands was detected using a Bio-Rad infrared gel imaging system (ChemiDoc XRS+).

### ***5-ethynyl-2'-deoxyuridine (EdU) incorporation assay***

Tumor cells were seeded on 24-well plates ( $1 \times 10^5$  cells/well), cultured for 48 h, and incubated with medium containing 50  $\mu$ M EdU (Beyotime, Shanghai, China) for 2 h. Cells were then fixed with 4% paraformaldehyde (Beyotime, Shanghai, China) and permeabilized, after which a click reaction mixture was added to the cells (200  $\mu$ L/well) for 30 min. Hoechst 33342 (200  $\mu$ L/well) staining for 30 minutes was performed to stain nuclei, and cells were visualized under a fluorescence microscope.

### ***Transwell migration and wound healing assays***

Cell migration and invasion were detected using Transwell chambers (BD, Franklin Lakes, NJ, USA) without and with a Matrigel coating, respectively, according to the manufacturer's instructions. After transfection,  $2 \times 10^5$  cells in serum-free medium were added to the upper chamber of the inserts, and medium containing 20% FBS was added to the lower chamber. After 24 h of culture, cells were fixed with 4% paraformaldehyde for 30 min, stained with crystal violet for 20 min and washed with phosphate-buffered saline (PBS). The cells were then counted under a microscope. The average number of cells in five fields of view on each membrane was counted three times.

For the wound healing assay, cells were plated in a 6-well plate, and then a scratch was created through a confluent cell layer with a sterile pipette tip. Debris was removed by washing the wells with PBS, and the cells were imaged immediately after scratching (baseline) and every 24 h thereafter.

### ***Laser confocal microscopy***

AGS and MGC803 cells treated with different compounds were seeded on coverslips in 24-well plates. Cells were fixed with 4% paraformaldehyde, incubated with 5% bovine serum albumin (BSA) (Sigma, Shanghai, China) for 30 min and stained with DAPI (Beyotime, Shanghai, China) for 7 min. The slides were air dried and sealed with a sealing tablet. LC3 fluorescence was observed under a confocal laser microscope, and the number of LC3 spots was counted

in 3 independent replicates.

### **Transmission electron microscopy**

Treated cells were trypsinized and collected after centrifugation. Then, they were fixed overnight with 2.5% phosphate-buffered glutaraldehyde (Sinopharm Chemical Reagents Co., Shanghai, China), after which they were embedded, sectioned, double stained with uranyl acetate and lead citrate and analyzed under a transmission electron microscope.

### **Establishment of tumor xenografts in CB17/SCID mice**

In all,  $3 \times 10^6$  cells in 100  $\mu$ L of PBS were subcutaneously injected into the right flanks of mice. The tumor growth rates were monitored by measuring the tumor diameter every 7 days, and the tumor volume was calculated using the following equation:  $1/2 LW^2$ , where L=length and W=width. The mice were treated with the indicated compounds 28 days later, and tumors were collected after gravimetric analysis.

### **Statistical analysis**

SPSS 19.0 software (SPSS Inc., IL, USA) was employed for all statistical analyses. Data are presented as the means  $\pm$  S.D. and were compared using Student's t-test or analysis of variance.  $P < 0.05$  was considered significant.

## **Results**

### **High FO XK1 expression predicts a poor prognosis for patients with GC**

FO XK1 expression in healthy stomach tissues and GC tissues was compared using GEPIA (Figure 1A), and we observed a significant increase in FO XK1 expression in GC tissues compared to that in healthy tissues. Additionally, the OS (Figure 1B) data obtained from the Kaplan-Meier plot were consistent with our curve created from data obtained from The Cancer Genome Atlas (TCGA), indicating that FO XK1 expression is associated with the survival of patients with GC. We next assessed FO XK1 expression in a TMA comprising 43 pairs of healthy control and GC tumor tissues from patients (Figure 1C). The tissue specimens were divided into a low FO XK1 expression group [immunoreactive score (IRS): 0–4] and

a high FO XK1 expression group (IRS: 4–12) based on a quantitative analysis of protein staining. We identified a correlation between the high FO XK1 expression group and the malignant progression of GC tissues (Figure 1D,E,  $P < 0.05$ ), as high FO XK1 expression was observed in 37 of 43 (86.0%) GC tissues (Table 1).

The clinical correlations between FO XK1 expression and the clinicopathological parameters of GC were further analyzed to explore the significance of FO XK1 upregulation (Table 1). High levels of FO XK1 were correlated with specific GC clinicopathological characteristics: pathological differentiation ( $P = 0.017$ ), microvascular tumor thrombus ( $P = 0.002$ ), lymph node metastases ( $P = 0.003$ ), tumor, node, metastasis (TNM) stage ( $P = 0.026$ ), and capsule invasion ( $P = 0.007$ ). FO XK1 expression was not correlated with sex, age, tumor location, or HER2 expression in the tumor. Taken together, these data clearly confirmed FO XK1 upregulation in GC tissues and the correlation of this increased expression with the degree of malignancy and clinical prognosis.

### **The effects of FO XK1 on GC cell proliferation**

Since elevated FO XK1 expression is correlated with malignant progression, FO XK1 may play an important role in one or more steps of GC proliferation. First, we further verified the increase in FO XK1 expression in GC cell lines using western blotting (Figure 2A). Increased protein levels of FO XK1 were detected in the AGS, SGC7901, BGC823, MGC803, and HGC27 cell lines compared to the normal human gastric cell line GES-1 (used as a control). Based on these results, we selected the AGS and MGC803 cell lines for further study because they exhibited a moderate increase in FO XK1 levels. AGS and MGC803 cells transfected with the pcDNA3.1-FO XK1 plasmid (FO XK1) were subsequently used in a proliferation assay, with cells transfected with an empty vector (vector) serving as a control. We also knocked down FO XK1 expression in AGS and MGC803 using an siRNA (Table S1) and compared its effects to those of control siRNAs. The transfection efficiency was validated using real-time PCR and western blotting (Figure 2B,C). Next, the results of the EdU assays suggested that FO XK1 overexpression markedly accelerated the growth of AGS and MGC803 cells, whereas downregulation of FO XK1 expression significantly reduced AGS and MGC803 proliferation (Figure 2D). Based on these findings, we can surmise that FO XK1 increases GC cell proliferation.

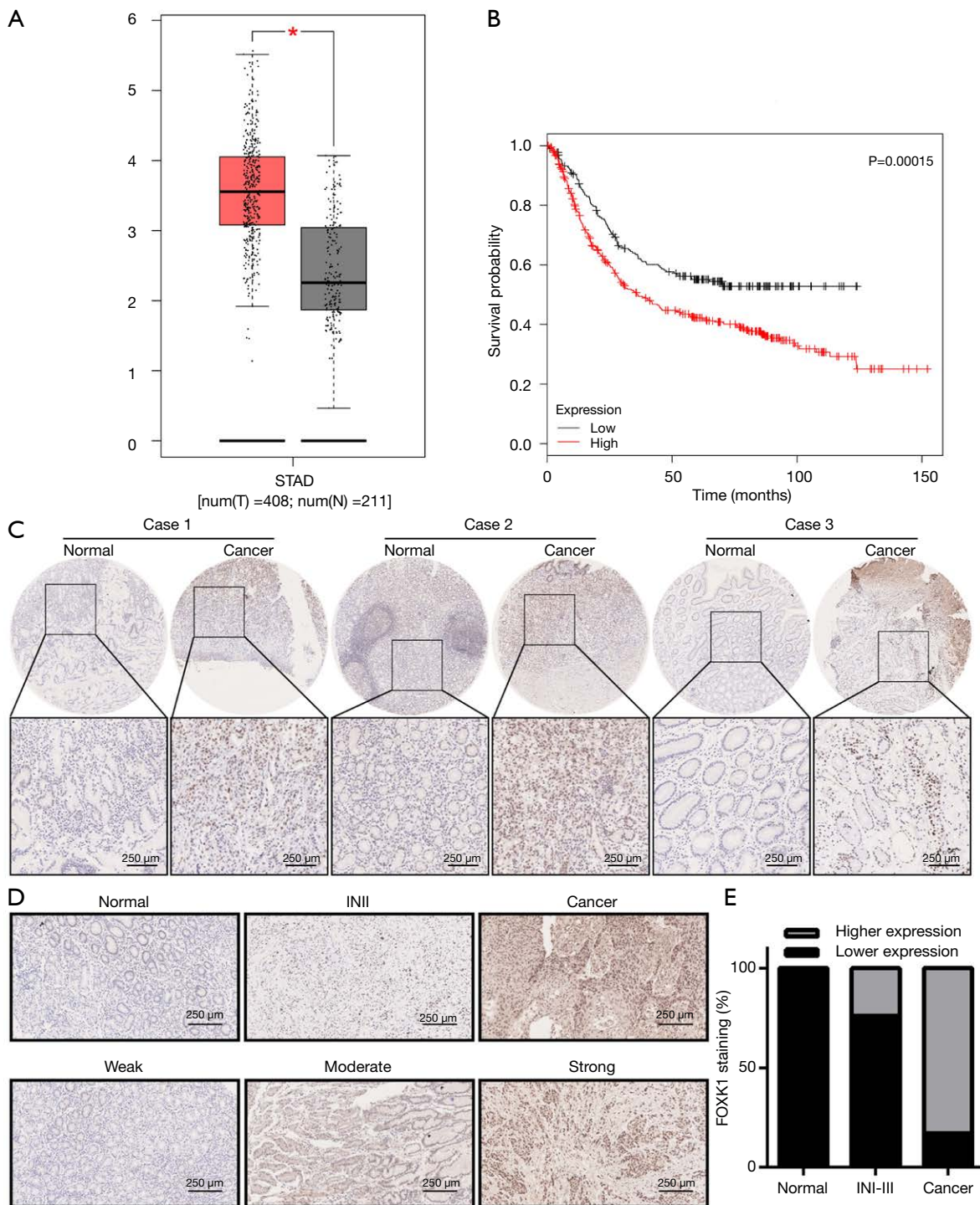


**Figure 1** High FOXX1 expression predicts a poor prognosis for patients with GC. (A) Boxplot of FOXX1 expression in GC based on GEPIA; (B) a Kaplan-Meier plot was used to analyze the prognosis of patients with GC stratified by FOXX1 expression (low FOXX1 expression group, n=221; high FOXX1 expression group, n=408); (C) FOXX1 expression in normal and malignant human gastric tissues was detected using IHC in TMA. Scale bar, 250 μm; (D) TMA of the levels of the FOXX1 protein in GC tissues. Representative images of FOXX1 staining by IHC in TMA. Scale bar, 250 μm; (E) FOXX1 expression increased with increasing malignant progression in GC. \*, P<0.05 and \*\*, P<0.01.

**Table 1** Correlation between FO XK1 expression and clinicopathological characteristics of patients with GC

Characteristics	Number	FO XK1 expression, n (%)		$\chi^2$	P value
		Low	High		
Gender				1.812	0.178
Male	34	3 (8.8)	31 (91.2)		
Female	9	3 (33.3)	6 (66.7)		
Age (years)				1.586	0.208
$\geq 60$	21	1 (4.8)	20 (95.2)		
<60	22	5 (22.7)	17 (77.3)		
Pathological differentiation				5.715	0.017*
Low	20	6 (30.0)	14 (70.0)		
High and moderate	23	0 (0)	23 (100)		
Microvascular tumor thrombus				9.898	0.002*
Present	28	0 (0.0)	28 (100.0)		
Absent	15	6 (40.0)	9 (60.0)		
Lymph node metastases				8.945	0.003*
Present	32	1 (3.1)	31 (96.9)		
Absent	11	5 (45.5)	6 (54.5)		
TNM stage				4.940	0.026*
I-II	15	5 (33.3)	10 (66.7)		
III-IV	28	1 (3.6)	27 (96.4)		
Capsule invasion				7.268	0.007*
Yes	35	2 (5.7)	33 (94.3)		
No	8	4 (50.0)	4 (50.0)		
Location of tumor				0.000	1
Antrum	27	4 (14.8)	23 (85.2)		
Non-antrum	16	2 (12.5)	14 (87.5)		
HER2 expression				0.000	1
Yes	20	3 (15.0)	17 (85.0)		
No	23	3 (13.0)	20 (87.0)		

\*, Statistically significant difference ( $P < 0.05$ ); continuity corrected using the  $\chi^2$  test.

### ***FO XK1 affects GC cell migration and invasion***

Because previous studies have reported a close association between FO XK1 expression and clinicopathological features, we evaluated the effects of FO XK1 on GC cell motility *in vitro*. Wound healing and Transwell assays were utilized to determine how FO XK1 influences GC cell migration and invasion. Based on the results from

the wound healing assays, FO XK1 overexpression led to increased motility compared with that of the control cells (*Figure 3A*). In contrast, FO XK1 knockdown in these same cells led to slower wound closure (*Figure 3B*). In Transwell assays, FO XK1 overexpression increased AGS and MGC803 cell migration and invasion compared with those of cells transfected with vector controls (*Figure 3C*).

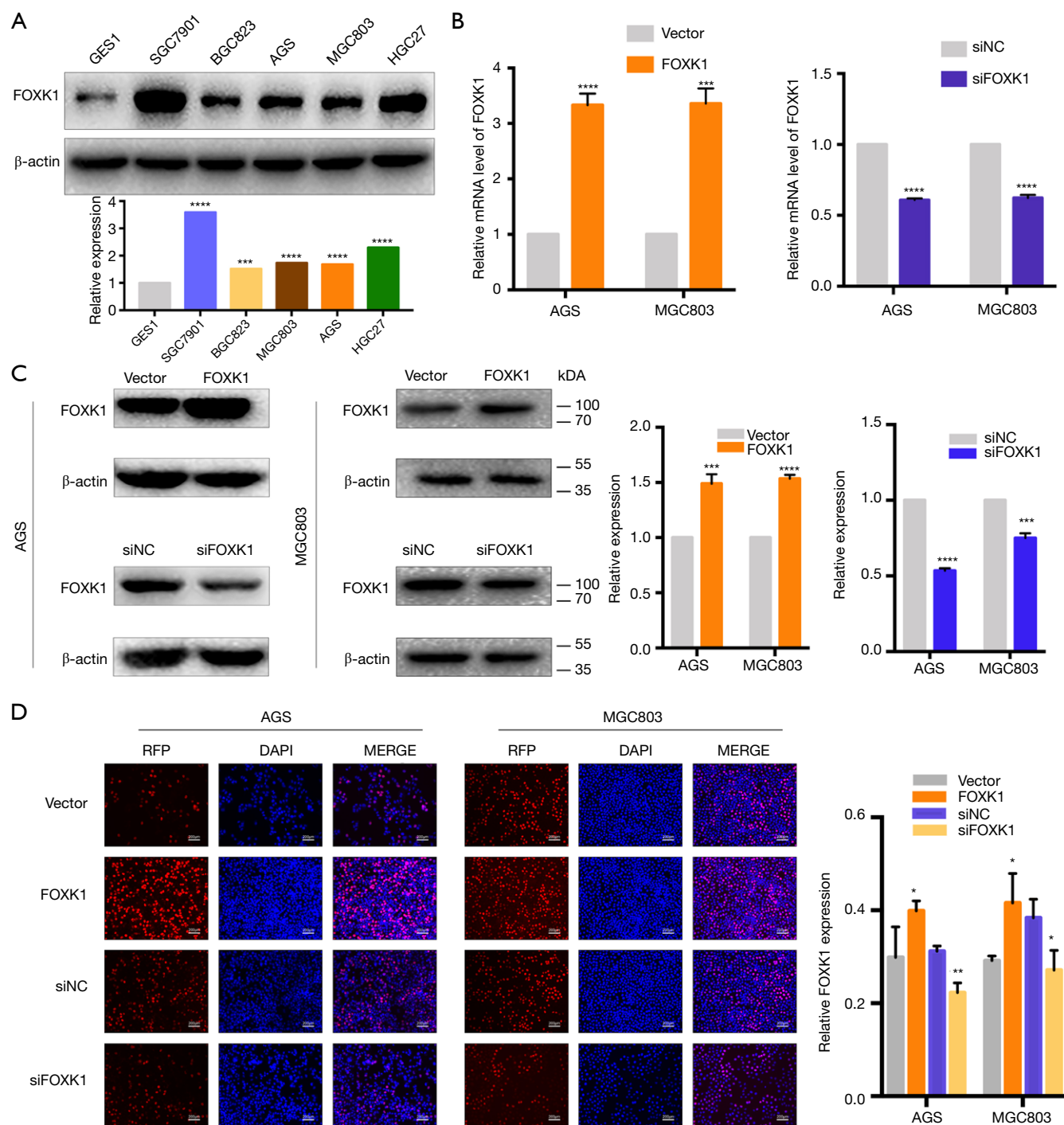


**Figure 2** FOXX1 promotes GC cell proliferation in vitro. (A) Protein levels of FOXX1 in normal GES1 cells and human GC cells were determined using western blotting; (B) transfection efficiency of FOXX1 overexpression and knockdown constructs, as measured by qRT-PCR; (C) transfection efficiency of the FOXX1 overexpression and knockdown constructs, as measured by western blotting; (D) DNA synthesis was measured by assessing EdU incorporation for 24 h, and the vector, FOXX1, siNC and siFOXX1 samples were compared. Scale bar, 200  $\mu$ m. The data are presented as the means  $\pm$  SD of three independent experiments. \*,  $P < 0.05$ , \*\*,  $P < 0.01$ , \*\*\*,  $P < 0.001$ , and \*\*\*\*,  $P < 0.0001$ .

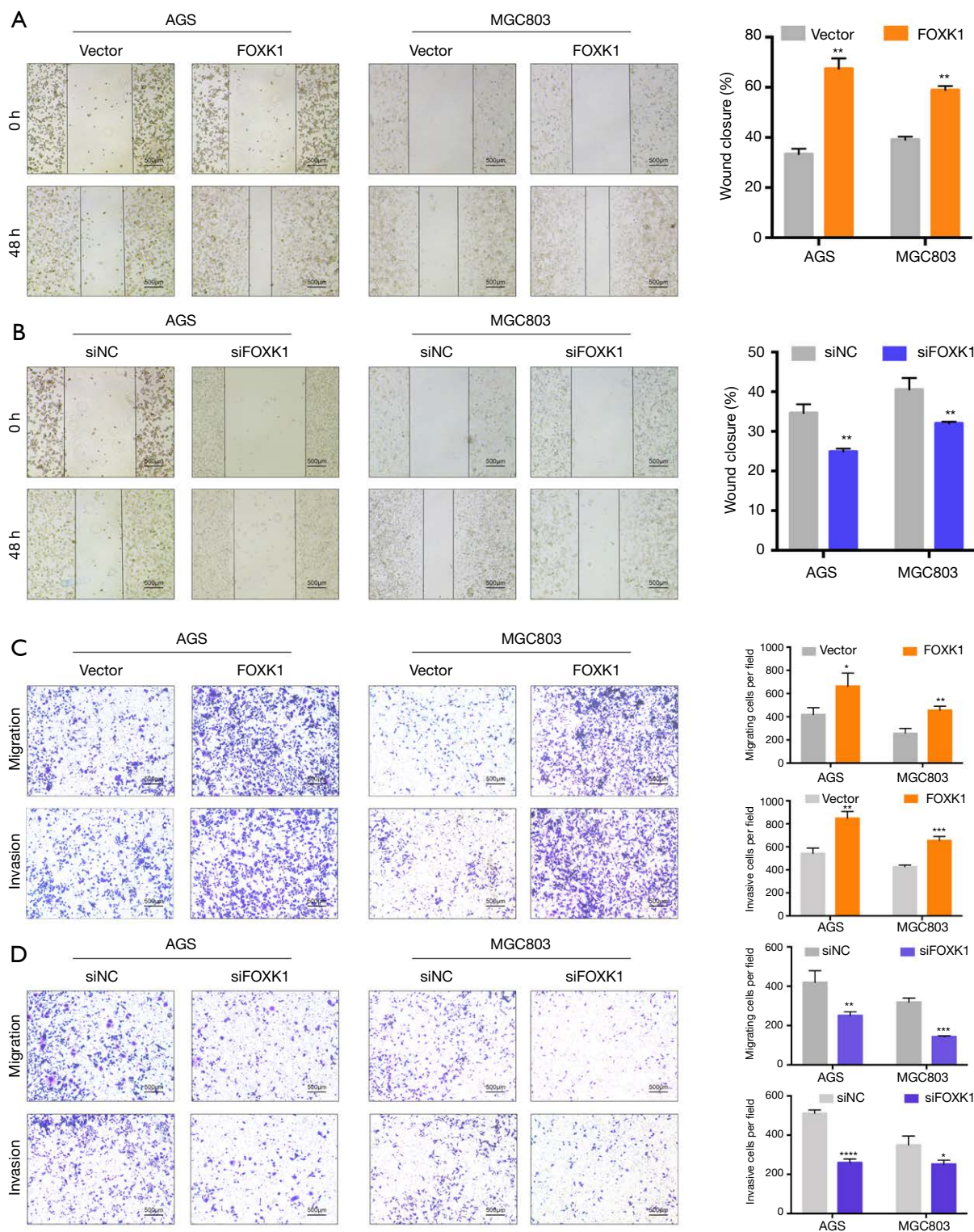


**Figure 3** FO XK1 promotes GC cell migration and invasion. (A,B) The motility of AGS and MGC803 cells was measured by examining wound closure following FO XK1 overexpression or knockdown. Scale bar, 500 μm; (C,D) Transwell assays were utilized to assess AGS and MGC803 cell migration and invasion following FO XK1 overexpression and knockdown. Scale bar, 500 μm. The data are presented as the means ± SD of three independent experiments. \*, P<0.05, \*\*, P<0.01, \*\*\*, P<0.001, and \*\*\*\*, P<0.0001.

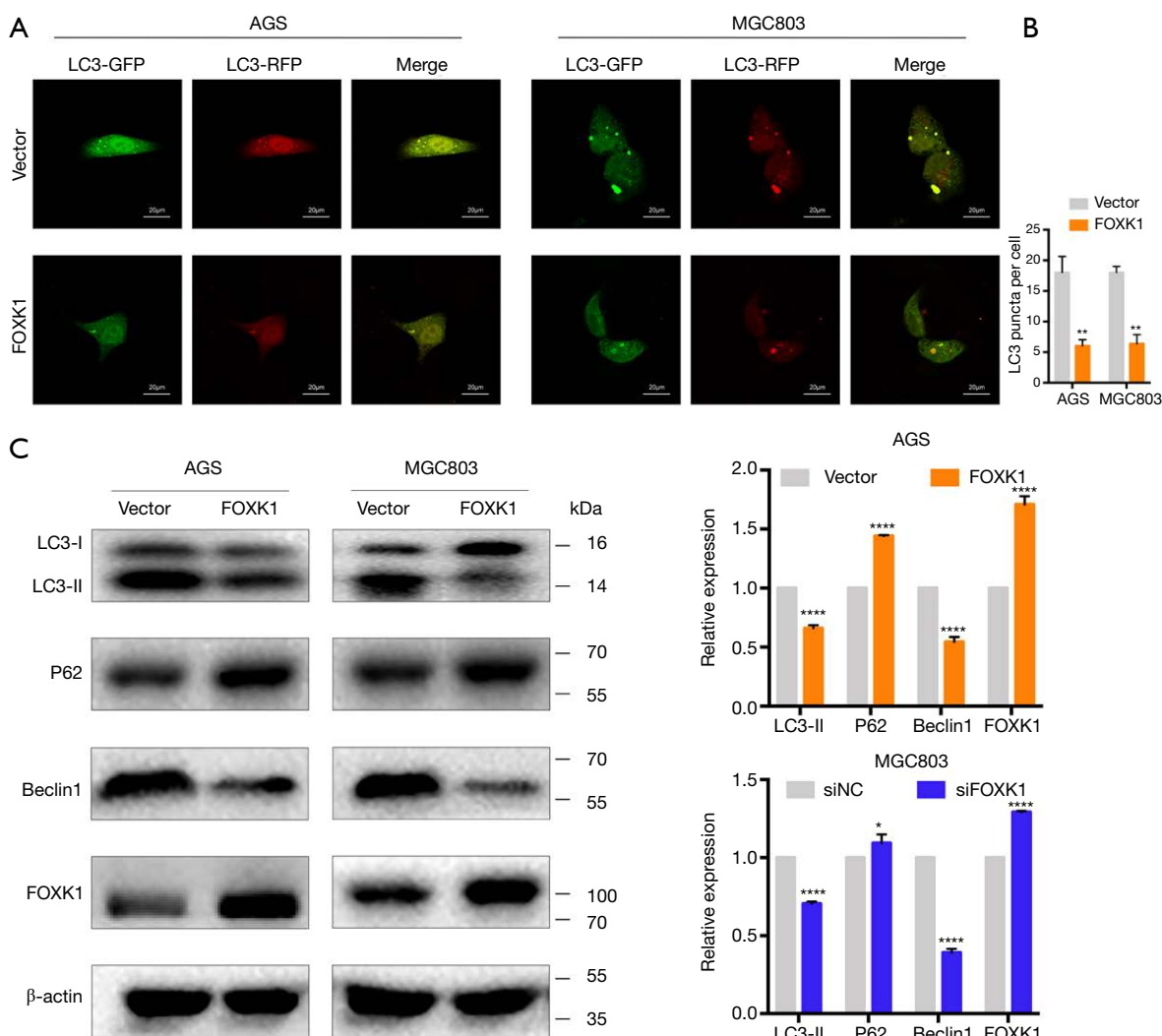


**Figure 4** FOXX1 suppresses autophagy in GC cells. (A,B) LC3 puncta in cells overexpressing FOXX1 were visualized under a confocal microscope after cells were subjected to immunofluorescence staining. Scale bar, 20  $\mu$ m; (C) the protein levels of LC3-I, LC3-II, p62, Beclin1 and FOXX1 were analyzed in FOXX1-transfected cells using western blotting. The data are presented as the means  $\pm$  SD of three independent experiments. \*,  $P < 0.05$ , \*\*,  $P < 0.01$ , and \*\*\*\*,  $P < 0.0001$ .

FOXX1 knockdown effectively reduced the number of invading cells in both cell lines (Figure 3D). FOXX1 thus drives the migration and invasion of GC cells *in vitro*.

#### FOXX1 suppresses autophagy in GC

Autophagy is closely linked to oncogenesis (14). Strategies that induce autophagy have been reported to inhibit tumor proliferation, invasion and migration (15,16). However, the relationship between FOXX1 expression and autophagy has not been previously reported in GC. To elucidate the

relationship between FOXX1 and autophagy, autophagy activity was assessed using a confocal laser imaging system. An emerging approach was used to analyze autophagosome-mediated dynamic changes in the protein levels and protein degradation. The functional switching of yellow fluorescence to red fluorescence reflects the functional autophagy flux after LC3 is fused in tandem with acid-resistant mCherry (such as RFP) and acid-sensitive GFP. As shown in Figure 4A,B, the yellow fluorescence of autophagic puncta was dramatically reduced in cells transfected with the pcDNA3.1-FOXX1 plasmid. Western blotting confirmed clear reductions in the

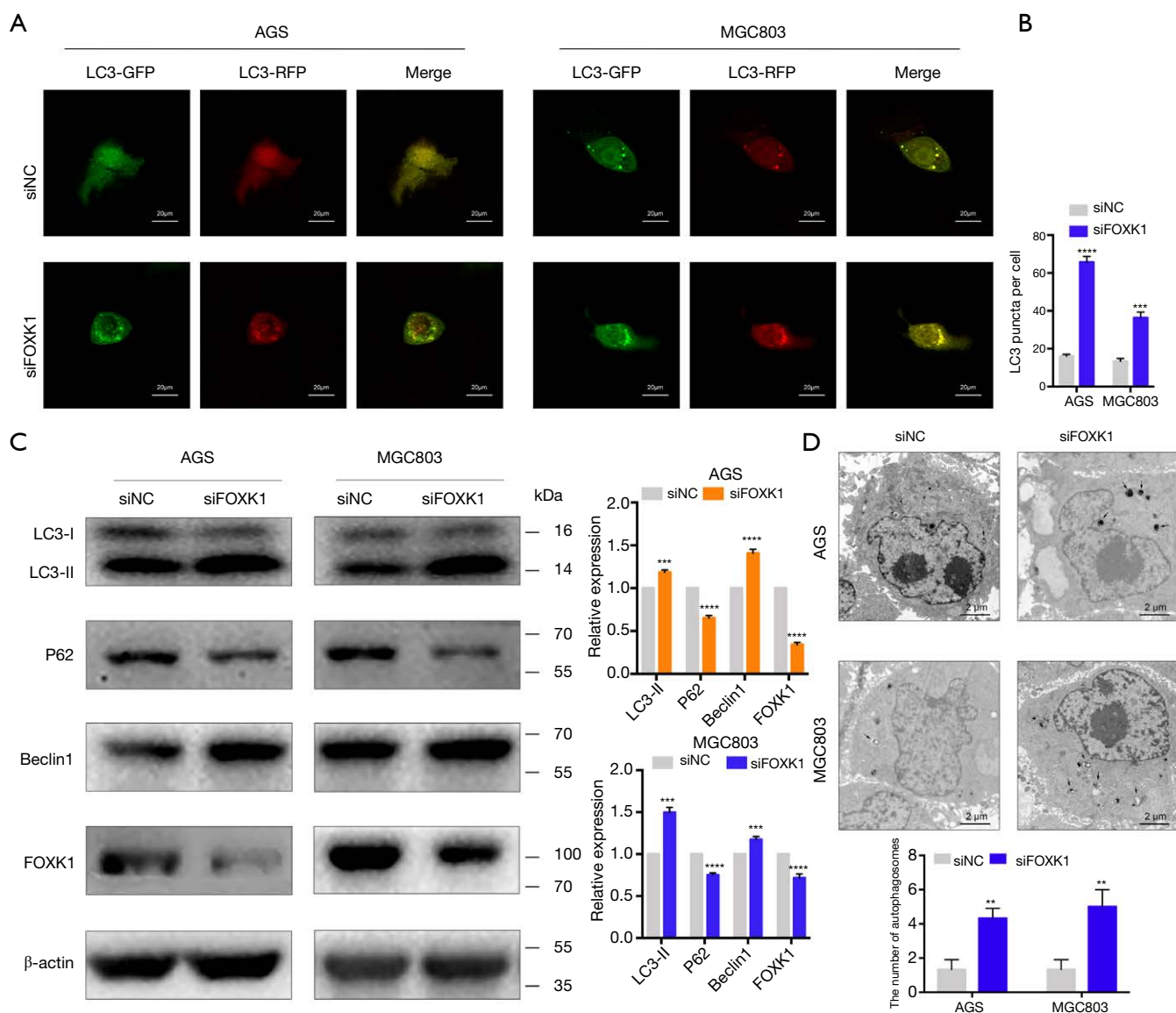


**Figure 5** FO XK1 knockdown promotes autophagy in GC cells. (A,B) LC3 puncta in cells transfected with siNC or siFOXK1 and subjected to immunofluorescence staining were visualized under a confocal microscope. Scale bar, 20  $\mu$ m; (C) the protein levels of LC3-II, p62, Beclin1 and FOXK1 were examined using western blotting in cells transfected with siNC or siFOXK1; (D) autophagosomes were observed under a transmission electron microscope in cells with FOXK1 knockdown. Scale bar, 2  $\mu$ m. The data are presented as the means  $\pm$  SD of three independent experiments. \*\*,  $P < 0.01$ , \*\*\*,  $P < 0.001$ , and \*\*\*\*,  $P < 0.0001$ .

expression levels of the autophagy-associated proteins LC3-II and Beclin1, as well as increased levels of p62 (Figure 4C).

#### FO XK1 knockdown promotes autophagy in GC cells

We assessed autophagy in cells with FOXK1 knockdown to further confirm the effect of FOXK1 on autophagy. The

results from the confocal laser analysis revealed a significant increase in autophagy following FOXK1 knockdown (Figure 5A,B), and western blotting confirmed clear increases in LC3-II and Beclin1 levels and decreased p62 levels (Figure 5C). Furthermore, transmission electron microscopy revealed autophagic vesicles containing engulfed organelles in the cytoplasm (Figure 5D).

### ***FOXK1 induces autophagy in GC cells by modulating the PI3K/AKT/mTOR signaling pathway***

The PI3K/AKT pathway was recently shown to function as a negative regulator of autophagy (17). Therefore, we used KEGG signaling pathway analysis to identify pathways that FOXK1 regulates and found that FOXK1 regulates PI3K activation (*Figure 6A*). Several other studies have shown that class I PI3K and class III PI3K have opposing functions in autophagy regulation (18). Therefore, we observed the effects of overexpression and knockdown of FOXK1 expression on class I PI3K, class III PI3K, AKT, and mTOR in GC cells. Western blots showed that levels of class I PI3K, the p-AKT/total AKT ratio and the p-mTOR/total mTOR ratio were significantly increased and that expression of class III PI3K was decreased after FOXK1 overexpression (*Figure 6B*). In addition, FOXK1 knockdown led to the opposite trend (*Figure 6C*). We also used real-time PCR to verify that FOXK1 can increase mRNA expression in class I PI3K, whereas the expression of class III PI3K is reduced (*Figure 6D*). Taken together, these data indicate that FOXK1 regulates autophagy at least in part through the PI3K/AKT/mTOR pathway. At the same time, FOXK1 inhibits autophagy by upregulating class I PI3K and downregulating class III PI3K.

### ***FOXK1 knockdown increases autophagy inhibited by 3-methyladenine (3-MA)***

3-MA, a class III phosphatidylinositol 3-kinase (PI3K) inhibitor, is currently the most widely used autophagy inhibitor (19). We transfected AGS and MGC803 cells with siNC and siFOXK1 to further determine the role of FOXK1 in the proliferation and invasion of cells in which 3-MA (200  $\mu$ m) suppressed autophagy. As shown in *Figure 7A*, in the presence or absence of 3-MA, LC3-II expression was increased and p62 expression was decreased after treatment with siFOXK1. Furthermore, western blotting results confirmed that the downregulation of LC3-II caused by 3-MA was enhanced by siFOXK1 in AGS and MGC803 cells. In contrast, upregulation of p62 induced by 3-MA was alleviated by siFOXK1. In addition, the results of the EdU and Transwell assays showed that silencing FOXK1 attenuated 3-MA-induced proliferation and invasion (*Figure 7B,C*). Based on these results, FOXK1 plays an important role in 3-MA-mediated suppression of autophagy in GC cells.

### ***Downregulation of FOXK1 inhibits GC growth in vivo***

We established mouse xenograft models to further examine the role of FOXK1 *in vivo*. First, LV-shNC and LV-shFOXK1 were transfected into MGC803 GC cells. Next, equal numbers of both groups of MGC803 cells were injected into the hind limbs of 4-week-old CB17/SCID mice. Four weeks after implantation, all the mice were sacrificed, and the tumor size and volume were recorded. As shown in *Figure 8A*, the tumors were significantly smaller in mice inoculated with LV-shFOXK1-transfected GC cells than in those inoculated with LV-shNC-transfected cells. Fifteen days after inoculation, the growth curve of the control group was significantly more pronounced than that of the LV-shFOXK1 group (*Figure 8B*). Accordingly, the xenografted tumors from the mice were weighed, and the tumors from the LV-shNC group were significantly heavier than those from the LV-shFOXK1 group (*Figure 8C*). As shown in *Figure 8D*, hematoxylin and eosin (H&E) staining confirmed the apparent heterogeneity of the cells in the tumor, with large nuclei and single staining. At the same time, western blotting analysis showed significantly reduced levels of FOXK1, class I PI3K, p-AKT, p-mTOR and p62 in tumors from mice in the LV-shFOXK1 group, which was accompanied by an increase in the level of class III PI3K and LC3-II (*Figure 8E*). Taken together, these data suggest that inhibiting FOXK1 expression increases autophagy levels in GC through the PI3K/AKT/mTOR pathway.

## **Discussion**

In this study, we analyzed the relationship between FOXK1 expression and clinicopathological features of GC patients. FOXK1 expression is closely correlated with the degree of GC malignancy. Subsequently, we determined that FOXK1 significantly affects the proliferation, invasion, and metastasis of GC cells and that autophagy may play a role in this process. Finally, FOXK1 was shown to activate the class I PI3K/AKT/mTOR pathway and inhibit class III PI3K, both of which block autophagy. Overall, FOXK1 represents a potential prognostic marker and a positive predictor of GC growth and invasiveness. Its upregulation promotes the malignant behavior of GC by inhibiting autophagy, and its mechanism may be related to the regulation of the PI3K/AKT/mTOR signaling pathway (*Figure S1*).

The FOX family of transcription factors is involved in tumorigenesis, tumor progression and embryogenesis

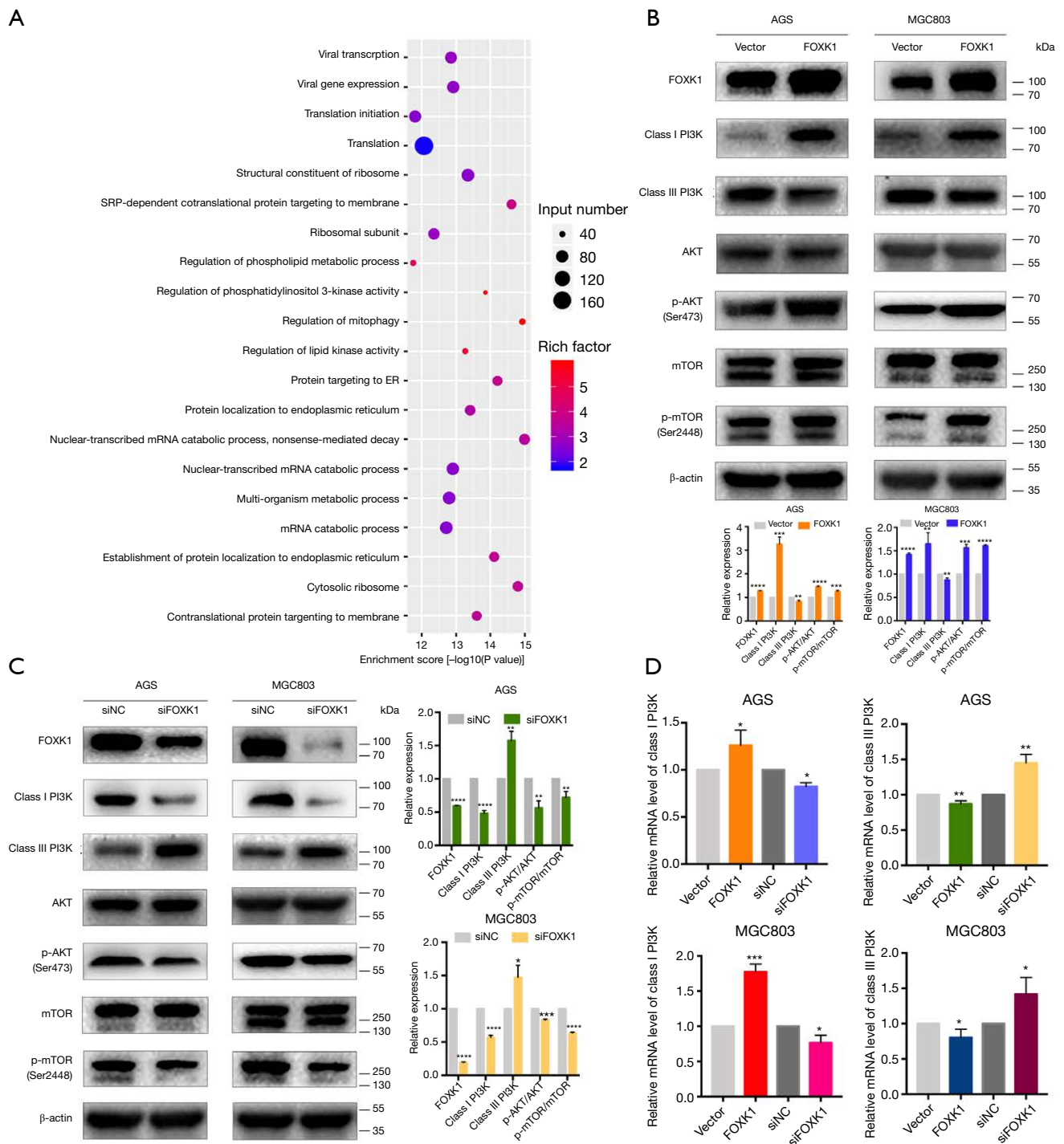


**Figure 6** FOXX1 induces autophagy in GC cells by modulating the PI3K/AKT/mTOR signaling pathway. (A) KEGG pathway analysis of FOXX1; (B) levels of FOXX1, class I PI3K, and class III PI3K and the ratios of p-AKT/total AKT and p-mTOR/total mTOR in GC cells overexpressing FOXX1 were assessed using Western blotting; (C) the protein levels of FOXX1, class I PI3K, class III PI3K, p-AKT/total AKT and p-mTOR/total mTOR in GC cells with FOXX1 knockdown were measured using western blotting; (D) FOXX1 overexpression and knockdown of the mRNA levels of class I PI3K and class III PI3K were assessed by qRT-PCR. The data are presented as the means  $\pm$  SD of three independent experiments. \*,  $P < 0.05$ , \*\*,  $P < 0.01$ , \*\*\*,  $P < 0.001$ , and \*\*\*\*,  $P < 0.0001$ .

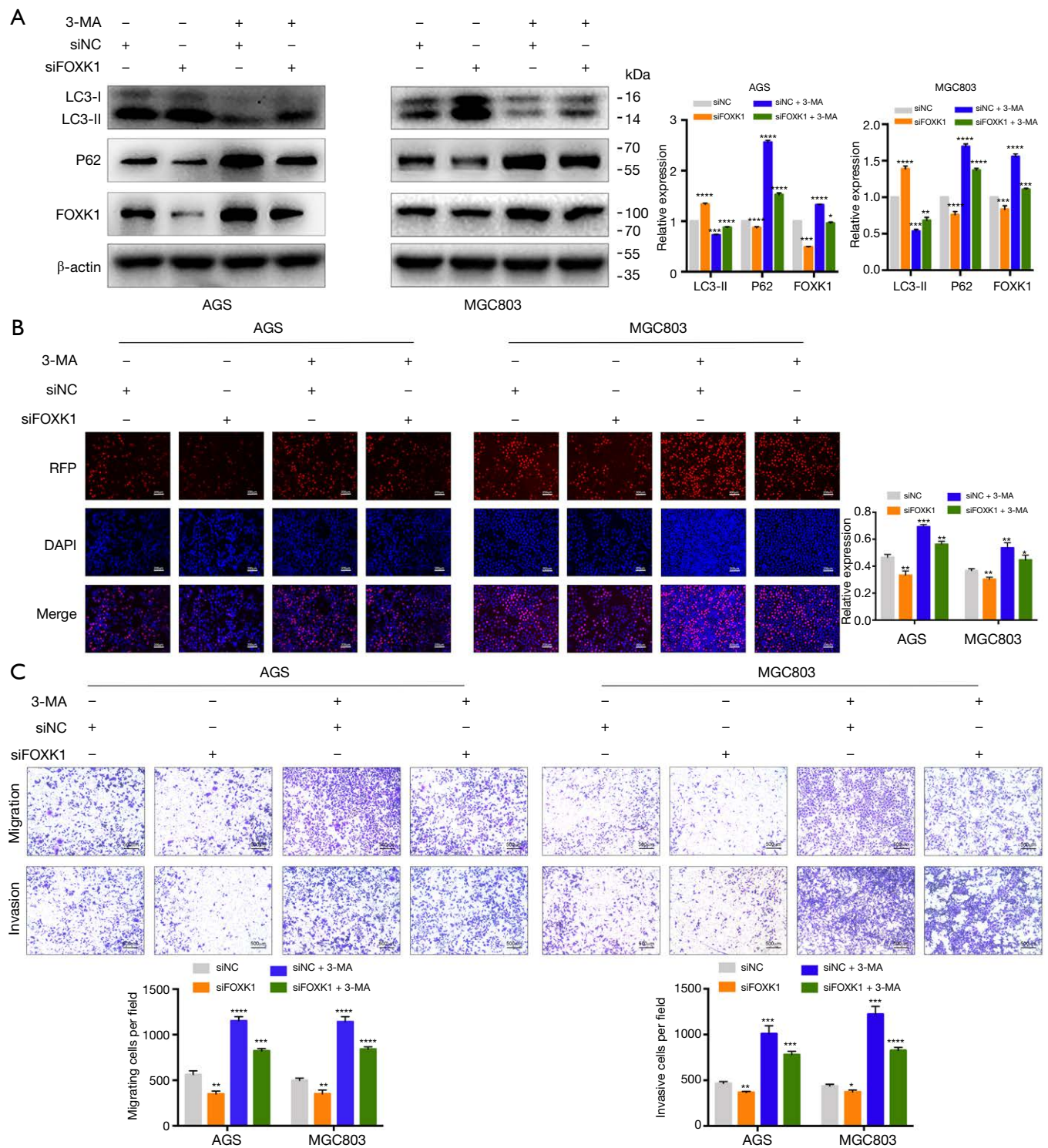


**Figure 7** FOXK1 knockdown increases autophagy inhibited by 3-MA. (A) After cells were transfected with siNC or siFOXK1, they were treated with 200  $\mu$ M 3-MA for 48 h. The levels of LC3-II, p62 and FOXK1 were detected using Western blotting; (B) representative images and analysis of EdU assays using AGS and MGC803 cells. Scale bar, 200  $\mu$ m; (C) invasion of cells treated with siNC, siFOXK1, siNC + 3-MA, and siFOXK1 + 3-MA. Scale bar, 500  $\mu$ m. The data are presented as the means  $\pm$  SD of three independent experiments. \*,  $P < 0.05$ , \*\*,  $P < 0.01$ , \*\*\*,  $P < 0.001$ , and \*\*\*\*,  $P < 0.0001$ .

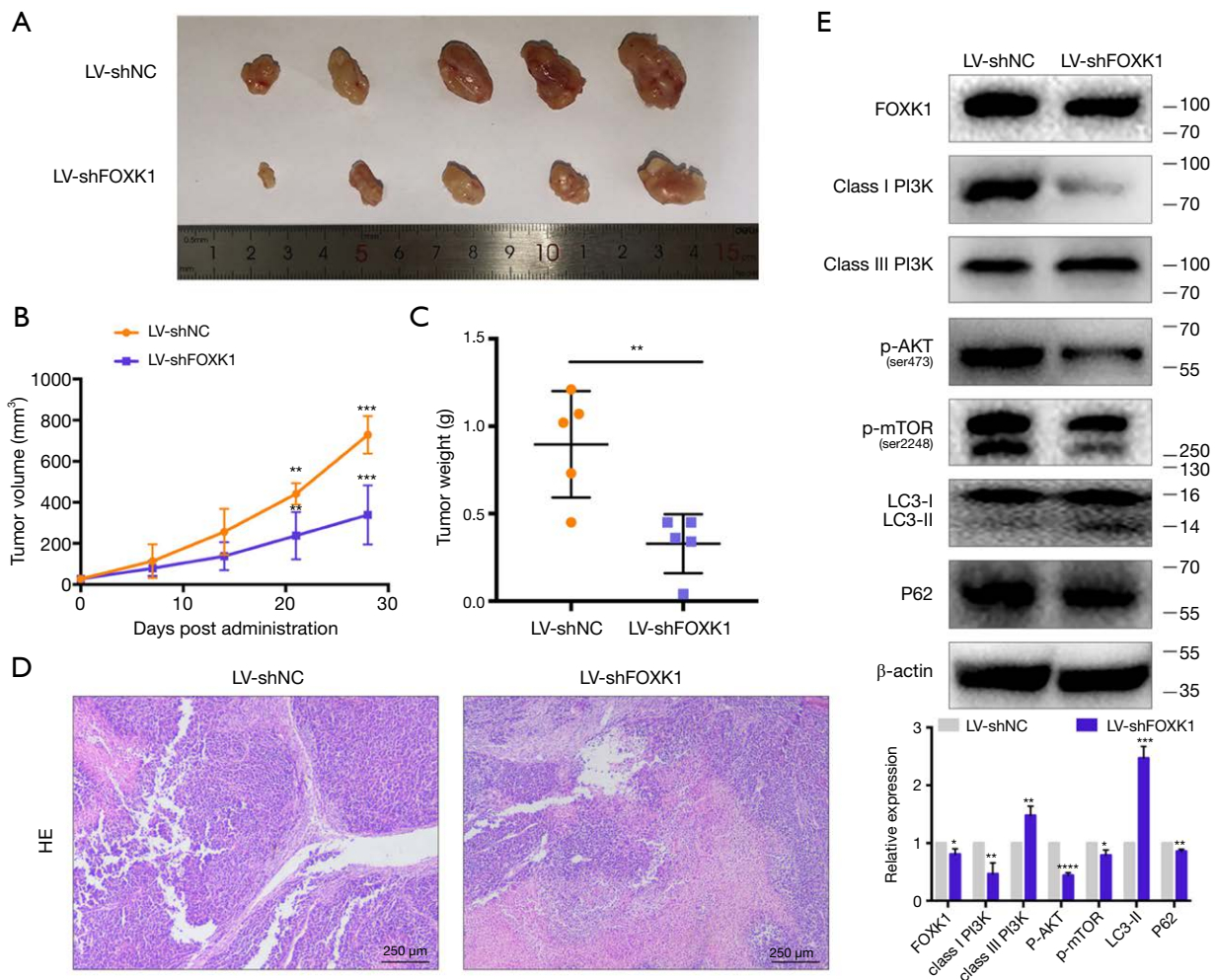


**Figure 8** Downregulation of FO XK1 inhibits GC growth in vivo. (A) Tumor tissues derived from xenograft tumors in CB17/SCID mice (n=6) 28 days after inoculation. Top panel, tumor derived from LV-NC-transfected cells; bottom panel, tumor derived from cells lacking FO XK1; (B) tumor growth curves for the LV-NC and LV-shFO XK1 groups. Tumor volumes were measured weekly; (C) the average tumor weights from mice in the LV-NC and LV-shFO XK1 groups. Tumors were excised at the end point of the experiment and weighed; (D) H&E staining of xenograft tumors from CB17/SCID mice; (E) levels of FO XK1, class I PI3K, class III PI3K, p-AKT, p-mTOR, LC3-II and p62 in tissues from xenograft tumors were detected using Western blotting. \*, P<0.05, \*\*P, <0.01, \*\*\*, P<0.001, and \*\*\*\*, P<0.0001.

(20,21). Based on accumulating evidence, FO XK1, a member of the FOX family, functions as an oncogene in many cancers when it is overexpressed. Wu *et al.* (22) also confirmed that FO XK1 interacts with FHL2 to promote colon cancer proliferation, invasion and metastasis. The abnormal expression of FO XK1 and consequent activation of downstream signaling pathways have been shown to lead to tumorigenesis and progression and alter the tumor phenotype. However, the mechanism by which FO XK1 promotes the malignant behavior of GC remains unclear. Our results confirm for the first time that FO XK1

overexpression increases proliferation and drives invasion and metastasis by inhibiting autophagy. Therefore, FO XK1 overexpression may be an important molecular target for cancer growth and metastasis, in which autophagy plays a key role.

Autophagy is a dynamic physiological process that aims to maintain cellular homeostasis. In some contexts, this process promotes cell survival by generating energy; however, this process changes drastically in tumors (23). Cancer cell-induced autophagy is more likely to be a dynamic mechanism that supports or inhibits tumor cell

survival. Chen HT and other scholars concluded that autophagy can act as a cancer suppressor and tends to prevent metastasis by selectively downregulating key transcription factors of EMT (24). According to a study by Kroemer, stress-induced hyperautophagy inhibits cell survival (16). As shown in a study by Wei R, inhibiting autophagy promotes the invasion and metastasis of colon cancer cells (15). Thus, autophagy represents a physiological process that can inhibit the proliferation and migration of tumor cells. Based on our results, FOXX1 overexpression decreases the LC3-II/LC3-I ratio and Beclin1 levels and increases p62 levels. After FOXX1 was knocked down, the LC3-II/LC3-I ratio and Beclin1 levels increased and p62 levels decreased, indicating that FOXX1 is a key factor regulating autophagy. This result is consistent with the findings reported by Christopher John Bowman (25). In the present study, the proliferation, invasion and metastasis of GC cell lines were increased after 3-MA-mediated inhibition of autophagy. Thus, FOXX1 may regulate autophagy during the later stages of tumor development, thereby promoting the malignant behaviors of GC.

The PI3K/AKT/mTOR signaling pathway plays a pivotal role in both development and disease, with a known role in cancer (26,27). PI3K is a member of a family of conserved lipid kinases whose aberrant activation is frequently observed in human cancers (28). Class I PI3K, which negatively regulate autophagy, phosphorylate PIP2 to produce PIP3. PIP3 recruits the second messenger AKT to send signals to mTOR to consequently inhibit autophagy (29,30). By contrast, class III PI3K drive processes that promote autophagy (18). In the present study, our results support the hypothesis that FOXX1 inhibits autophagy at least in part through the PI3K/AKT/mTOR signaling pathway to promote malignant behavior of tumors. Based on these findings, FOXX1 plays an important role in mediating GC progression, which provides new insights into further understanding and developing GC-based therapies.

## Conclusions

In summary, FOXX1 inhibits autophagy by activating the PI3K/AKT/mTOR pathway and inhibiting class III PI3K activity, thereby promoting the malignant behaviors of GC. These data reveal a new molecular mechanism of FOXX1 and autophagy in GC. In addition, FOXX1 may be a key factor predicting tumor progression and clinical outcomes in patients with GC. Therefore, the FOXX1-autophagy axis

represents a potential novel target for treating GC.

## Acknowledgments

We would like to thank M. Z. and Y. Q. for providing constructive suggestions and participating in discussions.

*Funding:* This study was supported by the Key Research and Development Foundation Projects of Shandong Province (2017GSF218109) and the Science and Technology Foundation Projects of Shandong Province (J15LL58).

## Footnote

*Conflicts of Interest:* The authors declare no conflicts of interest.

*Ethical Statement:* The authors are accountable for all aspects of this work in ensuring that questions related to the accuracy or integrity of any part of this work are appropriately investigated and resolved. The Medical Ethics Committee of Qingdao University and the Affiliated Hospital of Qingdao University approved the collection of clinical materials for research purposes. All samples were collected and analyzed after obtaining written informed consent from each patient. All animal experiments adhered to the Principles of Care and Use of Laboratory Animals of Qingdao University and were approved by the Subcommittee on the Ethics of Experimental Animal Welfare within the Medical Ethics Committee of Qingdao University (approval no. AHQDMAL20181201, approval date: 1 December 2018).

## References

1. Ang TL, Fock KM. Clinical epidemiology of gastric cancer. *Singapore Med J* 2014;55:621-8.
2. Lazăr DC, Tăban S, Cornianu M, et al. New advances in targeted gastric cancer treatment. *World J Gastroenterol* 2016;22:6776-99.
3. Wang J, Li W, Zhao Y, et al. Members of FOX family could be drug targets of cancers. *Pharmacol Ther* 2018;181:183-96.
4. Wolf I, Bose S, Williamson EA, et al. FOXA1: Growth inhibitor and a favorable prognostic factor in human breast cancer. *Int J Cancer* 2007;120:1013-22.
5. Sturgill TW, Stoddard PB, Cohn SM, et al. The promoter for intestinal cell kinase is head-to-head with F-Box 9 and contains functional sites for TCF7L2 and FOXA factors.

- Mol Cancer 2010;9:104.
6. Ma J, Matkar S, He X, et al. FOXO family in regulating cancer and metabolism. *Semin Cancer Biol* 2018;50:32-41.
  7. Fu W, Ma Q, Chen L, et al. MDM2 acts downstream of p53 as an E3 ligase to promote FOXO ubiquitination and degradation. *J Biol Chem* 2009;284:13987-4000.
  8. Shi X, Wallis AM, Gerard RD, et al. Foxk1 promotes cell proliferation and represses myogenic differentiation by regulating Foxo4 and Mef2. *J Cell Sci* 2012;125:5329-37.
  9. Li L, Gong M, Zhao Y, et al. FOXK1 facilitates cell proliferation through regulating the expression of p21, and promotes metastasis in ovarian cancer. *Oncotarget* 2017;8:70441-51.
  10. Xu H, Huang S, Zhu X, et al. FOXK1 promotes glioblastoma proliferation and metastasis through activation of Snail transcription. *Exp Ther Med* 2018;15:3108-16.
  11. Qian HR, Yang Y. Functional role of autophagy in gastric cancer. *Oncotarget* 2016;7:17641-51.
  12. Wang LL, Zhang L, Cui XF. Downregulation of long noncoding RNA LINC01419 inhibits cell migration, invasion, and tumor growth and promotes autophagy inactivation of the PI3K/Akt1/mTOR pathway in gastric cancer. *Ther Adv Med Oncol* 2019;11:1758835919874651.
  13. Cui H, Gao Q, Zhang L, et al. Knockdown of FOXK1 suppresses liver cancer cell viability by inhibiting glycolysis. *Life Sci* 2018;213:66-73.
  14. Galluzzi L, Pietrocola F, Bravo-San Pedro JM, et al. Autophagy in malignant transformation and cancer progression. *EMBO J* 2015;34:856-80.
  15. Wei R, Xiao Y, Song Y, et al. FAT4 regulates the EMT and autophagy in colorectal cancer cells in part via the PI3K-AKT signaling axis. *J Exp Clin Cancer Res* 2019;38:112.
  16. Kroemer G, Mariño G, Levine B. Autophagy and the integrated stress response. *Mol cell* 2010;40:280-93.
  17. Maejima Y, Kyoj S, Zhai P, et al. Mst1 inhibits autophagy by promoting the interaction between Beclin1 and Bcl-2. *Nat Med* 2013;19:1478-88.
  18. Li J, Zhou J, Zhang D, et al. Bone marrow-derived mesenchymal stem cells enhance autophagy via PI3K/AKT signalling to reduce the severity of ischaemia/reperfusion-induced lung injury. *J Cell Mol Med* 2015;19:2341-51.
  19. You P, Wu H, Deng M, et al. Brevilin A induces apoptosis and autophagy of colon adenocarcinoma cell CT26 via mitochondrial pathway and PI3K/AKT/mTOR inactivation. *Biomed Pharmacother* 2018;98:619-25.
  20. Pellegrini P, Strambi A, Zipoli C, et al. Acidic extracellular pH neutralizes the autophagy-inhibiting activity of chloroquine: implications for cancer therapies. *Autophagy* 2014;10:562-71.
  21. Teh MT, Wong ST, Neill GW, et al. FOXM1 Is a Downstream Target of Gli1 in Basal Cell Carcinomas. *Cancer Res* 2002;62:4773.
  22. Wu M, Wang J, Tang W, et al. FOXK1 interaction with FHL2 promotes proliferation, invasion and metastasis in colorectal cancer. *Oncogenesis* 2016;5:e271.
  23. Levy JM, Towers CG, Thorburn A. Targeting Autophagy in Cancer. *Nature reviews Cancer* 2017;17:528-42.
  24. Chen HT, Liu H, Mao MJ, et al. Crosstalk between autophagy and epithelial-mesenchymal transition and its application in cancer therapy. *Mol Cancer* 2019;18:101.
  25. Bowman CJ, Ayer D, Dynlacht B. Foxk proteins repress the initiation of starvation-induced atrophy and autophagy programs. *Nat Cell Biol* 2014;16:1202-14.
  26. Shayesteh L, Lu Y, Kuo WL, et al. PIK3CA is implicated as an oncogene in ovarian cancer. *Nat Genet* 1999;21:99-102.
  27. Levine DA, Bogomolny F, Yee CJ, et al. Frequent Mutation of the PIK3CA Gene in Ovarian and Breast Cancers. *Clin Cancer Res* 2005;11:2875-8.
  28. Yuan TL, Cantley LC. PI3K pathway alterations in cancer: variations on a theme. *Oncogene* 2008;27:5497-510.
  29. Saleh SN, Albert AP, Large WA. Activation of native TRPC1/C5/C6 channels by endothelin-1 is mediated by both PIP3 and PIP2 in rabbit coronary artery myocytes. *J Physiol* 2009;587:5361-75.
  30. van Rheenen J, Song X, van Roosmalen W, et al. EGF-induced PIP2 hydrolysis releases and activates cofilin locally in carcinoma cells. *J Cell Biol* 2007;179:1247-59.

**Cite this article as:** Wang Y, Qiu W, Liu N, Sun L, Liu Z, Wang S, Wang P, Liu S, Lv J. Forkhead box K1 regulates the malignant behavior of gastric cancer by inhibiting autophagy. *Ann Transl Med* 2020;8(4):107. doi: 10.21037/atm.2019.12.123

## Supplementary

**Table S1** FOXX1 siRNA sequence

FOXX1 siRNA	Sequence
Sense (5'-3')	CAACCUCUCUUUGAACCGUTT
Antisense (5'-3')	ACGGUJCAAAGAGAGGUUGTG

**Table S2** Antibodies used for Western blotting observation

Antibody	Dilution	Supplier	Item number
FOXX1	1/1,000	Cell Signaling Technology	#12025
LC3	1/1,000	Cell Signaling Technology	#4108
Beclin1	1/1,000	Bioworld	AP6020
$\beta$ -Actin	1/5,000	HuaBio	EM21002
SQSTM1/P62	1/1,000	Cell Signaling Technology	#5114
AKT	1/1,000	Cell Signaling Technology	#9272
mTOR	1/1,000	Cell Signaling Technology	#2972
p-AKT	1/1,000	Cell Signaling Technology	#9271
Class I PI3K	1/1,000	Cell Signaling Technology	#4228
Class III PI3K	1/1,000	Cell Signaling Technology	#13857
p-mTOR	1/1,000	Cell Signaling Technology	#2971

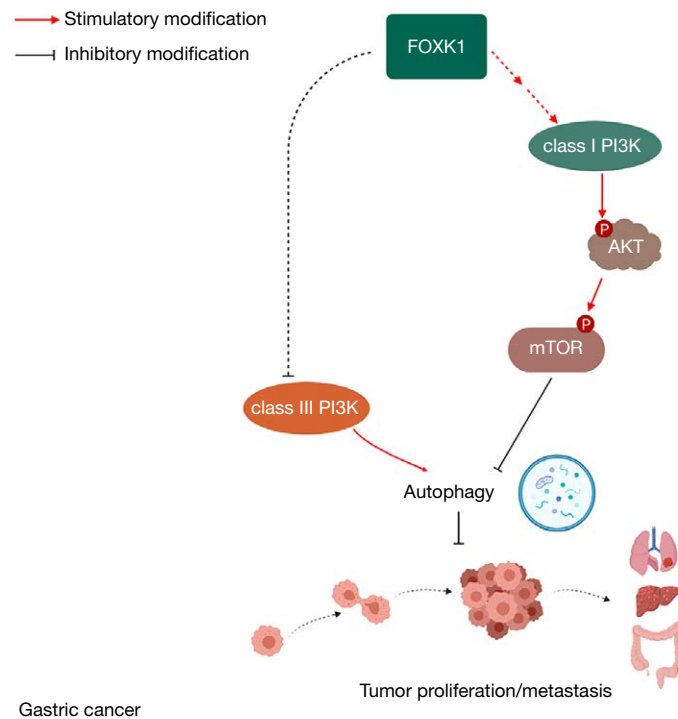


**Figure S1** The proposed mechanistic model of FOXX1 in gastric cancer. FOXX1 activates the PI3K/AKT/mTOR pathway in gastric cancer to inhibit autophagy and promote tumor growth, invasion and metastasis.